

Real-time imaging of histone H4 hyperacetylation in living cells

Kazuki Sasaki^a, Tamaki Ito^{a,b}, Norikazu Nishino^c, Saadi Khochbin^{d,e}, and Minoru Yoshida^{a,b,f,1}

^aChemical Genetics Laboratory/Chemical Genomics Research Group, RIKEN Advanced Science Institute, Wako, Saitama 351-0198, Japan; ^bGraduate School of Science and Engineering, Saitama University, Saitama, Saitama 338-8570, Japan; ^cGraduate School of Life Science and Systems Engineering, Kyushu Institute of Technology, Kitakyushu 808-0196, Japan; ^dInstitut National de la Santé et de la Recherche Médicale, U823, F-38706 Grenoble, France; ^eInstitut Albert Bonniot, Université Joseph Fourier, F-38700 Grenoble, France; and ^fJapan Science and Technology Corporation, CREST Research Project, Kawaguchi, Saitama 332-0012, Japan

Edited by Tom Misteli, National Cancer Institute, Bethesda, MD, and accepted by the Editorial Board July 30, 2009 (received for review March 2, 2009)

To visualize histone acetylation in living cells, we developed a genetically encoded fluorescent resonance energy transfer (FRET)-based indicator. Response of the indicator reflects changes in the acetylation state of both K5 and K8 in histone H4. Using this acetylation indicator, we were able to monitor the dynamic fluctuation of histone H4 acetylation levels during mitosis, as well as acetylation changes in response to structurally distinct histone deacetylase inhibitors.

BRDT | chromatin | FRET | HDAC inhibitor

Covalent modification of core histones plays an important role in the modulation of chromatin structure and function. Acetylation is a well-characterized modification regulated by two families of evolutionarily conserved enzymes, histone acetyltransferases (HATs) and histone deacetylases (HDACs) (1, 2). Acetylation mainly occurs on lysine residues of core histone N-terminal tails; in this context, the modification induces chromatin conformational change by unfolding higher order chromatin structure, and represents an epigenetic mark recognized by regulatory factors including coactivators. Core histone acetylation influences gene expression by modifying chromatin conformation and/or the recruitment of the regulatory factors. The acetylation of histone H4 is thought to occur initially at K16, and then propagates through K12, K8, and K5, progressing in an N-terminal direction (3). Thus, the simultaneous acetylation of both K5 and K8 in histone H4 is indicative of histone H4 hyperacetylation (4, 5). Acetylated histones are recognized by regulatory proteins containing bromodomains, for example, PCAF, Brd2, Brd4, and BRDT (6). Recently, it has been suggested that each distinct combination of covalent modifications of histone tails functions as an epigenetic code by regulating the interaction of histone tails with chromatin-associated proteins (7).

In vivo histone acetylation is reversibly and dynamically regulated. However, in most studies on protein acetylation, conventional biochemical methods such as immunostaining have been used. These methods do not always provide enough information about the temporal and spatial dynamics of protein acetylation in living cells. In the case of other cellular dynamics, such as intracellular Ca^{2+} and protein phosphorylation, visualization by fluorescence resonance energy transfer (FRET) in live cells has been used to successfully overcome the limitations of conventional methods (8). Here, we report a FRET-based indicator, named Histac, developed to allow visualization of protein acetylation in living cells.

Results

A Fluorescent Indicator for Histone H4 Hyperacetylation. For use as an indicator, we developed a five-part tandem fusion protein consisting of an acetylation-binding domain, a flexible linker, a substrate histone H4, and the two different-colored mutants of GFP (CFP and Venus), which serve as the donor and acceptor fluorophores, respectively, for FRET (Fig. 1A).

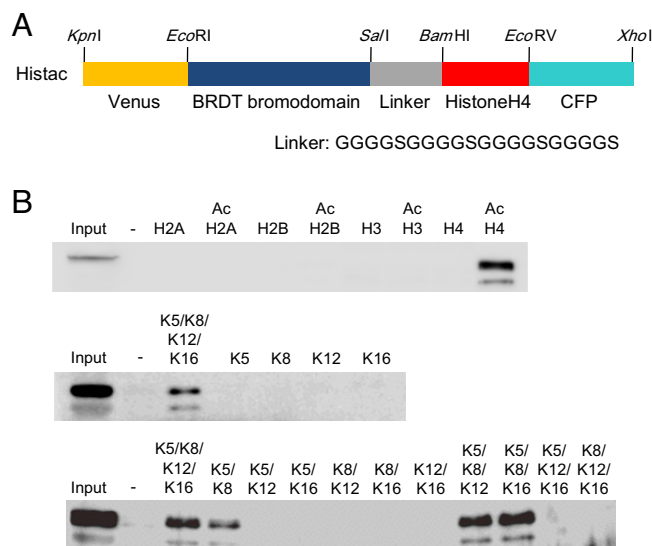


Fig. 1. (A) Schematic representation of the domain structure of Histac. (B) Peptide pull-down assay using nonmodified or acetylated (Ac) histone H4 N-terminal tail peptides (upper panel), or partly acetylated peptides (middle and lower panels). Pull-downs were analyzed by immunoblotting using an antibody against GFP.

Acetylation of the substrate histone H4 and subsequent binding of the acetylated substrate histone H4 to the acetylation-binding domain induce a conformational change in the indicator protein. The acetylation-dependent conformational change in the indicator alters the distance and orientation between CFP and Venus, thus generating a change in intramolecular FRET. The bromodomain region of BRDT, which contains two bromodomains, was used as the acetylation-binding domain (9). The peptide pull-down analysis revealed that this bromodomain region specifically bound to histone H4 peptides in which both K5 and K8 were acetylated (Fig. 1B). We constructed 13 potential indicators containing various Venus mutants with different domain organizations, and evaluated their ability to change the 480 nm/535 nm emission ratio in response to trichostatin A (TSA) (10), a potent inhibitor of HDACs, in live cells (Fig. S1). Among the candidates, six proteins showed the desired changes. We chose one, which we subsequently named Histac, for further study.

Author contributions: K.S. designed research; K.S. and T.I. performed research; N.N. and S.K. contributed new reagents/analytic tools; K.S. analyzed data; and K.S., S.K., and M.Y. wrote the paper.

The authors declare no conflict of interest.

This article is a PNAS Direct Submission. T.M. is a guest editor invited by the Editorial Board.

¹To whom correspondence should be addressed. E-mail: yoshidam@riken.jp.

This article contains supporting information online at www.pnas.org/cgi/content/full/0902150106/DCSupplemental.

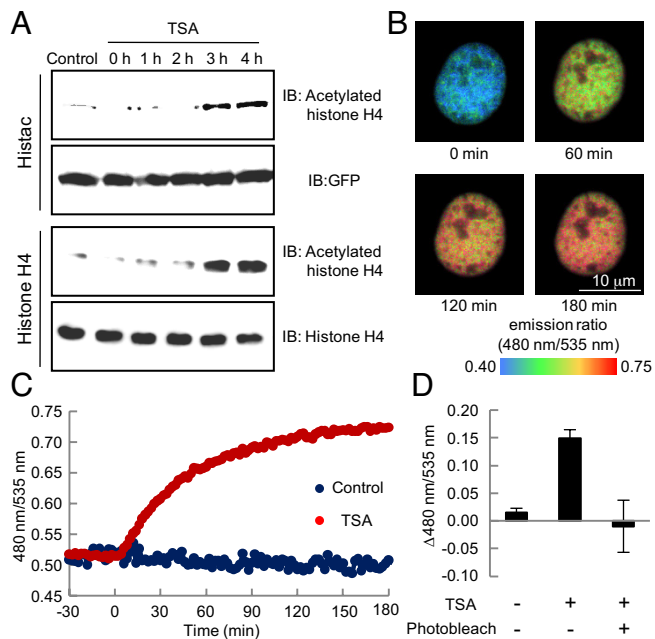


Fig. 2. (A) COS7 cells expressing Histac and nontransfected COS7 cells were treated with 1 μ M TSA. Immunoblot analyses were performed with antibodies against histone H4 acetylated at Lys-5, 8, 12, and 16. (B and C) Pseudocolored images and a time course of the emission ratio in the nucleus of a COS7 cell expressing Histac. TSA at a final concentration of 1 μ M or vehicle alone was added to the culture at 0 min. (D) After photobleaching of Venus within Histac, the cells were treated with 1 μ M TSA for 3 h.

Histac colocalized with nuclear DNA stained by Hoechst 33342 in COS7 cell (Fig. S2A). The ratios of fluorescence intensities between DNA and Venus determined at a number of distinct chromatin regions were essentially the same, suggesting that Histac is uniformly incorporated into chromatin (Fig. S2B). On the other hand, a mutant lacking the C-terminal globular domain of histone H4 (Histac- Δ C-H4) was located in both the nucleoplasm and the cytoplasm (Fig. S3A). To further investigate whether Histac was incorporated into nucleosomes, we fractionated extracts of the cells expressing Histac. Immunoblot analysis of cytoplasmic (Cy), nucleoplasmic (Nu), and chromatin (Ch) fractions showed that Histac was localized in the chromatin fraction, whereas Histac- Δ C-H4 was present in both the cytoplasmic and the nucleoplasmic fractions, indicating that the histone H4 globular domain is responsible for its chromatin association (Fig. S2C). In addition, we examined the effect of Histac expression on chromatin structure by determining the nucleosome repeat length. No difference between COS7 cells expressing Histac and the untransfected cells or those expressing Histac- Δ C-H4 was detected in the micrococcal nuclease digestion patterns (Fig. S2D).

We next verified acetylation of Histac by immunoblot analysis. The acetylation could be detected within 3 h after the COS7 cells expressing Histac were challenged with TSA (Fig. 2A). The time course showed a similar kinetics of acetylation to that of endogenous histone H4. In contrast, Histac- Δ C-H4 was hardly acetylated in response to TSA treatment (Fig. S3B), suggesting that, as with endogenous histones, incorporation into the nucleosomes is required for the efficient acetylation of Histac.

Fig. 2B and Movie S1 show images of a COS7 cell expressing Histac after TSA challenge: the 480 nm/535 nm emission ratio is expressed as pseudocolored images. The response reached a plateau within 3 h after TSA treatment (Fig. 2C). The length of time required for reaching the plateau was similar to that for

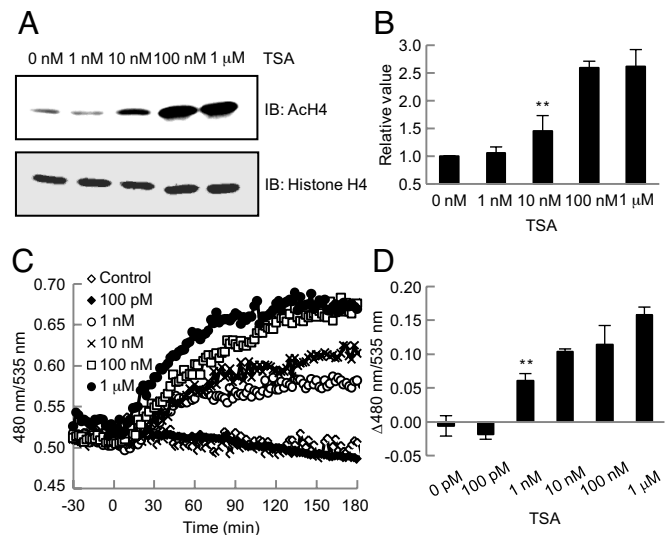


Fig. 3. Immunoblot analysis was performed with antibodies against histone H4 acetylated at Lys-5, 8, 12, and 16. COS7 cells were treated with various concentrations of TSA at 37 $^{\circ}$ C for 3 h (A and B). Emission ratio time courses (C) and changes in emission ratios (D) of cells expressing Histac treated with TSA. Asterisk indicates $P < 0.05$ compared with vehicle.

acetylation of Histac, as determined using immunoblotting (Fig. 2A and C). After the removal of TSA from the culture, both emission ratio and acetylation of Histac rapidly returned to the basal levels, indicating that Histac is a reversible indicator for monitoring acetylation of histone H4 in living cells (Fig. S4 and Movie S2). The cellular response in HeLa cells was essentially the same as in COS7 cells (Fig. S5). Photobleaching of Venus resulted in an increase in CFP fluorescence (Fig. S6), and the photobleached indicator no longer responded to TSA (Fig. 2D). These results confirm that the change in emission ratio reflects the change in FRET from CFP to Venus.

To detect changes in acetylation levels by immunoblot, a minimum dose of 10 nM TSA is required (Fig. 3A and B). In contrast, the minimum concentration of TSA required to induce the significant emission ratio change was approximately 1 nM (Fig. 3C and D). Thus, Histac is more sensitive in detecting histone acetylation than immunoblot analysis.

Mutational Analysis of the Acetylation-Binding Domain. To confirm that the TSA-induced change in FRET is a result of the binding of acetylated histone H4 domain to the acetylation-binding domain, we examined the effects of mutations in the Histac acetylation-binding domain (Fig. 4A). When two tyrosine residues were replaced with alanine in the acetylation-binding domain (2YA), the double-bromodomain mutant became incapable of binding to acetylated histone H4 (Fig. 4B) and failed to respond to TSA (Fig. 4C). The single Y65A mutant in bromodomain 1 was also impaired in its ability to bind to acetylated histone H4 (Fig. 4B) and did not show any detectable change in the emission ratio upon TSA treatment (Fig. 4C). In contrast, the Y308A mutant in bromodomain 2 retained the ability to bind to acetylated histone H4 (Fig. 4B) and showed a marked emission ratio change in response to TSA (Fig. 4C). No significant difference in the FRET response was observed between Histac and Histac-Y308A, suggesting that the major domain for recognizing acetylated histone H4 in BRDT is bromodomain 1.

Mutational Analysis of Acetylation Sites. To verify that the TSA-induced change in FRET reflects acetylation at the specific sites

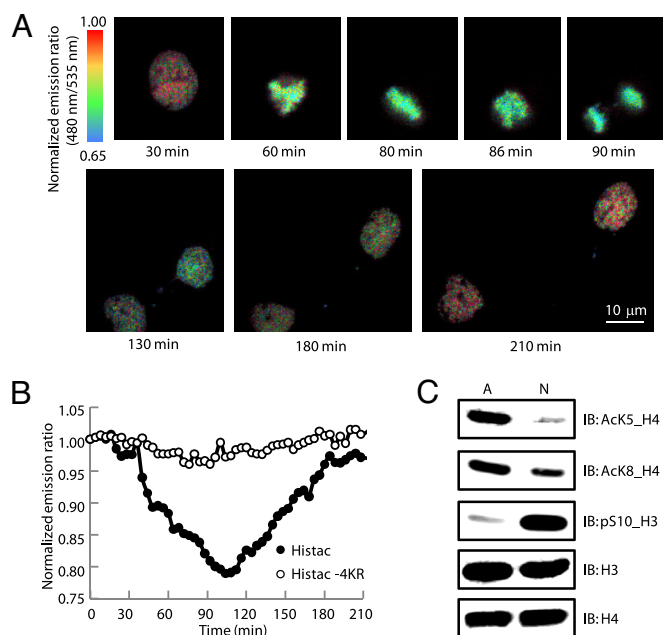


Fig. 6. (A) Pseudocolored images of the 480 nm/535 nm emission ratio obtained from a COS7 cell expressing the acetylation indicator during mitosis. (B) Time courses of the 480 nm/535 nm emission ratio of Histac (●) and Histac-4KR (○) during mitosis. (C) Acetylation of histone H4 at K5 and K8 of asynchronous (A) and nocodazole-treated (N) COS7 cells was analyzed by immunoblotting using antibodies against histone H4 acetylated at K5 and K8. Phosphorylated histone H3 (pS10), a mitotic marker, was analyzed by immunoblotting using an antibody against phosphorylated histone H3. COS7 cells were arrested in mitosis by treatment with 10 μ g/mL nocodazole for 12 h.

(Fig. S9B). This observation suggests the existence of distinct regions with different HDAC activities in the nucleus.

Evaluation of HDAC Inhibitors in Living Cells. Histac is a highly sensitive imaging probe for monitoring the activity of HDAC inhibitors in living cells. FK228, which is currently studied clinically (18), is another potent HDAC inhibitor. FK228 has an intramolecular disulfide bond, and is activated in cells by reduction to form two sulfhydryl groups, one of which can interact with the HDAC active site (19). It was unclear, however, how much time is required for this process. Using Histac, we detected FK228 activity immediately after the challenge (Fig. 7A), indicating that FK228 is rapidly incorporated and activated in the cells. CHAP31 (20) and SCOP402 (21), cyclic tetrapeptides having a hydroxamic acid and a disulfide as functional groups, respectively, also showed rapid FRET responses (Fig. 7B and C). In contrast, SCOP304 (21), a dimer form of SCOP152 with a disulfide, gave significantly different kinetics (Fig. 7D). It showed a delayed response onset, and took more time than other HDAC inhibitors to reach a plateau, probably due to poor membrane permeability. Based on these inhibitor data, it is clear that Histac serves as a powerful assay tool for *in vivo* HDAC inhibitor action.

Discussion

Before the existence of Histac, Kanno et al. (22) developed a method to screen for bromodomains that interact with acetylated histone, using a flow cytometric adaptation of FRET termed FC-FRET. This approach enabled one to measure the steady-state interaction between bromodomain proteins and acetylated histones in living cells. However, because the state of histone acetylation is thought to be dynamically regulated in the cell, a real-time imaging probe for *in vivo* histone acetylation has

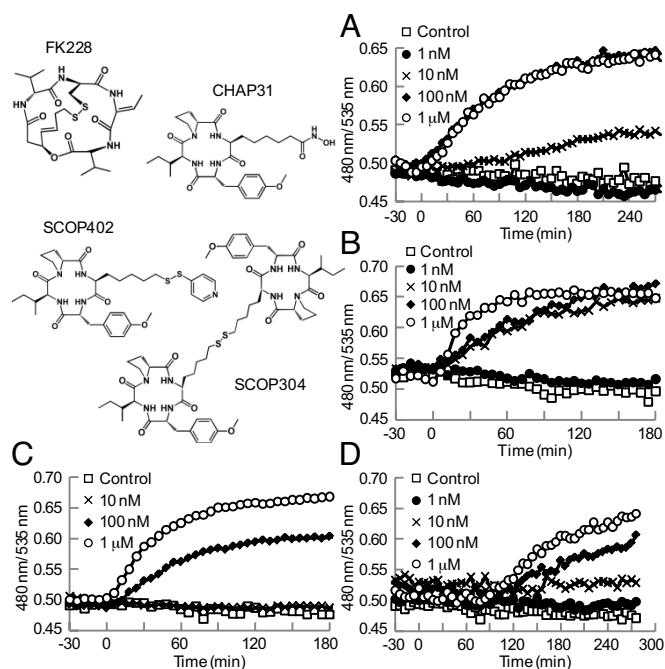


Fig. 7. Emission ratio time courses of cells expressing Histac treated with (A) FK228, (B) CHAP31, (C) SCOP402, and (D) SCOP304. Each HDAC inhibitor was added to the culture at 0 min.

been long awaited. In this study, we showed that a FRET probe fused tandemly with the BRDT bromodomain and histone H4 enabled us to visualize the dynamic changes in histone H4 acetylation in living cells. Indeed, we could demonstrate the decrease in the level of histone H4 K5/K8 acetylation at metaphase. Although early observation suggested no significant change in acetylation of histone H4 K5, recent analyses using immunofluorescence staining, immunoblotting, and mass spectrometry demonstrated the opposite (14–16). The present study verified the dramatic decrease in K5 acetylation in mitosis. In immunofluorescence staining it cannot be ruled out that an antibody might be inaccessible to acetylated histones during mitosis, due to chromatin condensation. Moreover, because cell synchronization is required for immunoblotting and mass spectrometry, stress induced by the agents for cell synchronization might affect the histone acetylation state. Histac can bypass these technical challenges.

It is unclear why Histac-4KR still responded, albeit weakly, to TSA-induced hyperacetylation of histone H4 (Fig. 5A). It seems possible that Histac may form a nucleosome together with an endogenous histone H4 molecule, and that the bromodomain in Histac-4KR can interact with acetylated lysine residues in the flexible tail of the endogenous histone H4 in the same nucleosome. The X-ray structure analysis of a nucleosome showed that histone H4 possesses an unstructured N-terminal tail, leaving the 13 N-terminal residues in one of the two H4 molecules and seven N-terminal residues in the other H4 disordered (23). The X-ray structure of the nucleosome (PDB ID: 1EQZ) indicates that the distance between the residues of the two structured H4 N-terminal ends in a nucleosome is approximately 7.6 nm. The bromodomain in Histac is fused to the flexible N-terminal extension from the structured end via a flexible 20-residue linker in which the length per residue is approximately 0.38 nm (24). Therefore, it seems likely that the flexible intervening polypeptide bridges the gap to allow access of the bromodomains to the acetylation sites of the endogenous H4.

In vitro pull-down experiments show a strict requirement for the acetylation at both K5 and K8 for the BRDT binding (Fig. 1B). This requirement appears less strict in vivo, because of the possible cross-talks between the bromodomain and acetylated K5 and K8 in the endogenous H4 in the same nucleosomes (Fig. 5A). The simultaneous presence of acetylation on both K5 and K8 is a signature of H4 hyperacetylation. A zip model supports the idea that acetylation propagates from K16 to K5 and simultaneous acetylation at K5 and K8 should therefore indicate hyperacetylated H4 (3–5). Thus, Histac is a unique probe for imaging hyperacetylated histone H4. In this study, we demonstrate that the K12 acetylation is required for the efficient K5 acetylation, which may be one of the mechanisms underlying the zip model. The acetylation of K12 may directly or indirectly facilitate the recruitment of a HAT to induce acetylation at K5 in mammalian cells.

The ability of Histac to recognize the in vivo histone H4 acetylation correlated well with the properties of the interaction of BRDT with histone H4 in vitro. BRDT contains two bromodomains. The bromodomain structure consists of an atypical left-handed four-helix bundle (helices α_Z , α_A , α_B , and α_C), a long intervening loop between helices α_Z and α_A (termed the ZA loop), and a loop between helices α_B and α_C (termed the BC loop) (6). The ZA and BC loops form a hydrophobic pocket, to which an acetyl-lysine residue binds. Y65 (bromodomain 1) and Y308 (bromodomain 2) in the ZA loops in the BRDT bromodomains are highly conserved throughout the large family of bromodomains, including GCN5, TAFII250, CBP, p300, and Brd2. We found that the substitution of alanine for Y65 in bromodomain 1 is sufficient to impair its ability to bind to acetylated histone H4. On the other hand, Y308A did not abolish the binding of BRDT to acetylated histone H4. These results suggest that bromodomain 1 in BRDT is the primary binding domain for acetylated histone H4, and bromodomain 2 is the secondary domain. This idea is consistent with the observation that BRDT containing a mutation in the bromodomain 1 (P50A, F51A, and V55A) could not induce chromatin remodeling, while BRDT containing a mutation in bromodomain 2 (P293A, F294A, and V298A) retained TSA-dependent chromatin remodeling activity (9).

In conclusion, we have developed an indicator for visualizing histone H4 acetylation in living cells. Since our indicator recognizes the acetylation of K5 and K8, the response reflects the hyperacetylation of histone H4 (3–5). It seems probable that exchange of the acetylation-binding domain with other bromodomains [e.g., Brd2 binds to acetylated K12 in histone H4 (22)] will allow monitoring of other acetylation sites. Our approach provides a tool for spatial and temporal analysis of protein acetylation, and will help to understand when, where, and how

histone H4 is acetylated in living cells, tissues, and transgenic animals.

Materials and Methods

Plasmid Construction, Cell Culture, and Transfection. The cDNA of ECFP, Venus, histone H4, bromodomains of BRDT (BRDT_{1–443}), and the linker were generated using PCR and cloned into the restriction sites shown in Fig. 1A. Each cDNA was subcloned into the *KpnI-XhoI* site of a mammalian expression vector, pcDNA3.1(+) (Invitrogen).

COS7 cells and HeLa cells were cultured in DMEM supplemented with 10% FCS, 1% penicillin/streptomycin, 1 mM sodium pyruvate, and 0.1 mM nonessential amino acids at 37 °C in 5% CO₂. These cells were transfected with a FuGENE 6 transfection reagent (Roche) and were then cultured for 24 h at 37 °C in 5% CO₂.

Imaging of Cells. After transfection, the culture medium was replaced with phenol red-free growth medium for imaging. Cells were observed at 37 °C in 5% CO₂ on an Olympus IX81 microscope with a UIC-QE cooled charged-coupled device camera (Molecular Devices). Images were collected by using a MetaFluor (Universal Imaging) with a 440AF21 excitation filter, a 455DRLP dichroic mirror, and two emission filters (480AF30 for CFP and 535AF26 for Venus). For Fig. S2, the images of Hoechst 33342 staining and Venus were collected with FV1000 (Olympus) confocal microscope system.

Gel Electrophoresis and Immunoblot Analysis. For Figs. 1B and 4B, peptide pull-down assays were performed as described by Pivot-Pajot et al. (9). COS7 cells were transiently transfected with monomeric Venus-BRDT or monomeric Venus-BRDT-mutants. For Fig. S2C, mononucleosome core particles were purified as described by Kanda et al. (25). The fractions were immunoprecipitated using an anti-GFP antibody (Takara Bio).

Immunoblot analysis was performed using standard procedures and visualized using ECL Western Blotting Detection Reagents (GE Healthcare Bio-Science Corp.). The antibodies that recognize acetyl-lysine 5, 8, 12, and 16, respectively, of histone H4 were obtained from Upstate Biotechnology. The anti-histone H3, anti-histone H4, anti-GFP, and anti-FLAG antibodies were purchased from Cell Signaling Technology, Abcam, Takara Bio, and Sigma, respectively. The anti-HDAC1 and anti-tubulin were obtained from Sigma.

Micrococcal Nuclease Digestion. Micrococcal nuclease digestion was carried out essentially as described by Remboutsika et al. (26). The nucleus of COS7 cells expressing the indicators were digested with increasing amounts of micrococcal nuclease (0.2, 0.8, or 3.2 units per 10⁷ nucleus) (Sigma) at 37 °C for 10 min. DNA was purified by phenol/chloroform extraction and ethanol precipitation, and separated in a 2% agarose gel.

ACKNOWLEDGMENTS. We thank Atsushi Miyawaki (RIKEN, Japan) for providing various Venus mutants and helpful discussion, A. Ganesan (University of Southampton and Karus Therapeutics Ltd., U.K.) for providing FK228, and Akihiro Ito for discussion; BSI's Research Resources Center for providing DNA sequencing analysis and peptide synthesis; and RIKEN BSI-Olympus Collaboration Center for imaging equipment and software. This work was supported in part by Grant-in-aid for Scientific Research on Priority Areas (to K.S.); CREST Research Project, JST, Grants-in-aid for Cancer Research from the Ministry of Education, Culture, Sports, Science, and Technology of Japan (to M.Y.), and "ANR blanc" "Episperm" & "Empreinte, INCA," and "ARC-ARECA" research programs (to S.K.).

- Khochbin S, Verdel A, Lemerrier C, Seigneurin-Berny D (2001) Functional significance of histone deacetylase diversity. *Curr Opin Genet Dev* 11:162–166.
- Yang X-J, Seto E (2007) HATs and HDACs: From structure, function and regulation to novel strategies for therapy and prevention. *Oncogene* 26:5310–5318.
- Thorne AW, Kmiecik D, Mitchelson K, Sautiere P, Crane-Robinson C (1990) Patterns of histone acetylation. *Eur J Biochem* 193:701–713.
- Zhang K, et al. (2002) Histone acetylation and deacetylation: Identification of acetylation and methylation sites of HeLa histone H4 by mass spectrometry. *Mol Cell Proteomics* 1:500–508.
- Garcia BA, et al. (2007) Organismal differences in post-translational modifications in histones H3 and H4. *J Biol Chem* 282:7641–7655.
- Zeng L, Zhou MM (2002) Bromodomain: An acetyl-lysine binding domain. *FEBS Lett* 513:124–128.
- Ruthenburg AJ, Li H, Patel DJ, Allis CD (2007) Multivalent engagement of chromatin modifications by linked binding modules. *Nat Rev Mol Cell Biol* 8:983–994.
- Miyawaki A (2003) Visualization of the spatial and temporal dynamics of intracellular signaling. *Dev Cell* 4:295–305.
- Pivot-Pajot C, et al. (2003) Acetylation-dependent chromatin reorganization by BRDT, a testis-specific bromodomain-containing protein. *Mol Cell Biol* 23:5354–5365.
- Yoshida M, Kijima M, Akita M, Beppu T (1990) Potent and specific inhibition of mammalian histone deacetylase both *in vivo* and *in vitro* by trichostatin A. *J Biol Chem* 265:17174–17179.
- Turner BM, Fellows G (1989) Specific antibodies reveal ordered and cell-cycle-related use of histone-H4 acetylation sites in mammalian cells. *Eur J Biochem* 179:131–139.
- Yoshida M, Beppu T (1988) Reversible arrest of proliferation of rat 3Y1 fibroblasts in both the G1 and G2 phases by trichostatin A. *Exp Cell Res* 177:122–131.
- Bolden JE, Peart MJ, Johnstone RW (2006) Anticancer activities of histone deacetylase inhibitors. *Nat Rev Drug Discov* 5:769–784.
- Kruhlik MJ, et al. (2001) Regulation of global acetylation in mitosis through loss of histone acetyltransferases and deacetylases from chromatin. *J Biol Chem* 276:38307–38319.
- Valls E, Sánchez-Molina S, Martínez-Balbás MA (2005) Role of histone modifications in marking and activating genes through mitosis. *J Biol Chem* 280:42592–42600.
- Bonenfant D, et al. (2007) Analysis of dynamic changes in post-translational modifications of human histones during cell cycle by mass spectrometry. *Mol Cell Proteomics* 6:1917–1932.
- Albiez H, et al. (2006) Chromatin domains and the interchromatin compartment form structurally defined and functionally interacting nuclear networks. *Chromosome Res* 14:707–733.

18. Schrump DS, et al. (2008) Clinical and molecular responses in lung cancer patients receiving Romidepsin. *Clin Cancer Res* 14:188–198.
19. Furumai R, et al. (2002) FK228 (depsipeptide) as a natural prodrug that inhibits class I histone deacetylases. *Cancer Res* 62:4916–4921.
20. Komatsu Y, et al. (2001) Cyclic hydroxamic-acid-containing peptide 31, a potent synthetic histone deacetylase inhibitor with antitumor activity. *Cancer Res* 61:4459–4466.
21. Nishino N, et al. (2003) Cyclic tetrapeptides bearing a sulfhydryl group potently inhibit histone deacetylases. *Org Lett* 5:5079–5082.
22. Kanno T, et al. (2004) Selective recognition of acetylated histones by bromodomain proteins visualized in living cells. *Mol Cell* 13:33–43.
23. Harp JM, Hanson BL, Timm DE, Bunick GJ (2000) Asymmetries in the nucleosome core particle at 2.5 Å resolution. *Acta Crystallogr D* 56:1513–1534.
24. Huston JS, et al. (1988) Protein engineering of antibody binding sites: Recovery of specific activity in an anti-digoxin single-chain Fv analogue produced in *Escherichia coli*. *Proc Natl Acad Sci USA* 85:5879–5883.
25. Kanda T, Sullivan KF, Wahl GM (1998) Histone-GFP fusion protein enables sensitive analysis of chromosome dynamics in living mammalian cells. *Curr Biol* 8:377–385.
26. Remboutsika E, et al. (1999) The putative nuclear receptor mediator TIF1 α is tightly associated with euchromatin. *J Cell Sci* 112:1671–1683.